NIH Public Access
Author Manuscript
Adv Healthc Mater. Author manuscript; available in PMC 2014 January 01.

Published in final edited form as:
Adv Healthc Mater. 2013 January ; 2(1): 195–205. doi:10.1002/adhm.201200194.

Directed Differentiation of Size-Controlled Embryoid Bodies Towards Endothelial and Cardiac Lineages in RGD-Modified Poly(Ethylene Glycol) Hydrogels

Lina Schukur,
Center for Biomedical Engineering, Department of Medicine, Brigham and Women's Hospital, Harvard Medical School, 02115, USA, Harvard-MIT Division of Health Sciences and Technology, Massachusetts Institute of Technology, 02139, USA, 65 Landsdowne Street Cambridge, MA 02139, USA

Institute of Biochemistry and Molecular Biology, Medical School, RWTH Aachen University, 52074, Germany

Pinar Zorlutuna,
Center for Biomedical Engineering, Department of Medicine, Brigham and Women's Hospital, Harvard Medical School, 02115, USA, Harvard-MIT Division of Health Sciences and Technology, Massachusetts Institute of Technology, 02139, USA, 65 Landsdowne Street Cambridge, MA 02139, USA

Jae Min Cha,
Center for Biomedical Engineering, Department of Medicine, Brigham and Women's Hospital, Harvard Medical School, 02115, USA, Harvard-MIT Division of Health Sciences and Technology, Massachusetts Institute of Technology, 02139, USA, 65 Landsdowne Street Cambridge, MA 02139, USA

Hojae Bae, and
Center for Biomedical Engineering, Department of Medicine, Brigham and Women's Hospital, Harvard Medical School, 02115, USA, Harvard-MIT Division of Health Sciences and Technology, Massachusetts Institute of Technology, 02139, USA, 65 Landsdowne Street Cambridge, MA 02139, USA

Ali Khademhosseini
Center for Biomedical Engineering, Department of Medicine, Brigham and Women's Hospital, Harvard Medical School, 02115, USA, Harvard-MIT Division of Health Sciences and Technology, Massachusetts Institute of Technology, 02139, USA, 65 Landsdowne Street Cambridge, MA 02139, USA

Wyss Institute for Biologically Inspired Engineering, Department of Medicine, Brigham and Women's Hospital, Harvard Medical School, 02115, USA

Ali Khademhosseini: alik@rics.bwh.harvard.edu

Abstract

Recent advances in stem cell research have demonstrated the importance of microenvironmental cues in directing stem cell fate towards specific cell lineages. For instance, the size of the

© 2013 WILEY-VCH Verlag GmbH & Co. KGaA, Weinheim

Correspondence to: Ali Khademhosseini, alik@rics.bwh.harvard.edu.

Supporting Information
Supporting Information is available from the Wiley Online Library or from the author.

NIH-PA Author Manuscript
NIH-PA Author Manuscript
NIH-PA Author Manuscript

NIH-PA Author Manuscript

NIH-PA Author Manuscript

NIH-PA Author Manuscript

embryoid body (EB) was shown to play a role in stem cell differentiation. Other studies have used cell adhesive RGD peptides to direct stem cell fate towards endothelial cells. In this study, materials and cell-based approaches are combined by using microwell arrays to produce size-controlled EBs and encapsulating the resulting aggregates in high molecular weight PEG-4 arm acrylate with and without conjugated RGD to study their effect on stem cell differentiation in a 3D microenvironment. Increasing EB size is observed along with a decrease in the total number of EBs in pristine PEG hydrogel, regardless of the initial EB size. In correlation with this aggregation, EBs in PEG show enhanced cardiogenic differentiation compared to RGD-PEG hydrogel. Both aggregation and cardiogenic differentiation are significantly reduced when RGD peptides are introduced to the microenvironment, while endothelial cell differentiation is accelerated by 3 to 5 days, depending on the EB size, and doubled over the course of cell culture for both EB sizes. Presented results indicate that RGD sequence has a dominant effect in driving endothelial cell differentiation in size-controlled EBs, while pristine multi-arm, high molecular weight PEG can induce cardiogenic differentiation, possibly through EB aggregation. The photopatternable nature of the hydrogel used in this study enabled patterning of such domains devoid or abundant of cell attachment sequences. Therefore, these hydrogels can potentially be used for spatially patterned embryonic stem cell differentiation, which may be beneficial for tissue engineering and regenerative medicine applications.

1. Introduction

Regeneration of complex tissues such as myocardium is of great interest in various regenerative medicine and drug discovery applications. In the past few years there have been numerous studies on designing scaffolds with the aim of creating a functional tissue that can be applied as a transplant in vivo.[1] So far, clinical applications of engineered tissues have been limited to poorly vascularized tissues such as cornea, skin or cartilage, while engineering complex and highly vascularized tissues remains a major challenge.[2] This is mostly due to lack of sufficient vasculature within the engineered tissues, which limits the access of cells to nutrition and oxygen.[3] Different strategies have been attempted to create vascularized engineered tissues to address this challenge.[4] One promising approach is based on inducing endothelial cells (ECs) to form capillaries or to create new angiogenic sprouts from pre-existing ones similar to their behavior during embryonic development.[5] To achieve this, embryonic stem cells (ES cells) are a potential cell source. ES cells have the ability to proliferate indefinitely and to differentiate into every somatic cell type of the body.[6, 7] The aggregation of ES cells into spheres called embryoid bodies (EBs) is one of the inducers for their differentiation into three germ layers: ectoderm, mesoderm, and endoderm. This ability makes ES cells an important target for a range of tissue engineering applications.[8] Despite the therapeutic potential of ES cells, there is a significant challenge to their medical application due to the inability to direct their differentiation into a defined cell type in a homogenous manner.[9]

It is becoming increasingly clear that the microenvironment plays a significant role in stem cell differentiation.[10] Understanding the influence of native microenvironment enables scaffold designs with biomimetic properties towards controlled stem cell differentiation. Recent advances in stem cell biology have began to elucidate some of the molecular interactions between the microenvironmental cues and the behavior and development of the cells and tissues.[11, 12] For instance, when ECs start sprouting during embryogenesis, they release factors such as matrix metalloproteinases (MMP), various cell adhesion proteins (i.e., fibronectin or laminin), growth factors and cytokines (i.e., vascular endothelial growth factor (VEGF), platelet-derived growth factor (PDGF)).[13] Influence of these microenvironmental factors, consisting of both surrounding cells and the extracellular matrix (ECM) is crucial in vasculogenesis and has attracted attention in tissue engineering

NIH-PA Author Manuscript

NIH-PA Author Manuscript

NIH-PA Author Manuscript

approaches.[14] Many research groups have designed ECM-mimetic synthetic hydrogel constructs by conjugating RGDS and MMP-sensitive sequences to poly(ethylene glycol) (PEG)-based hydrogels.[15–17] In this way, cell adhesion properties and degradability can be directly engineered in the materials, which can be used for creating environments for improved vasculogenesis.

Another important parameter in ES cell differentiation that can alter the surrounding microenvironment is the size of the ES cell aggregates.[18] In our previous studies, we have demonstrated that the differentiation of ES cells can be regulated to a certain extend by controlling the size of the EBs.[19] In particular, when size-controlled cell aggregates seeded on cell culture dishes, endothelialization was enhanced in smaller EBs (150 μm diameter), while larger EBs (450 μm diameter) differentiated towards cardiomyocytes.

In this study, we further elaborated on this promising result by combining this behavior with engineered materials. Using the same microwell array technique to create size controlled EBs before encapsulation, different-sized EBs (i.e., 150 μm and 450 μm in diameter) were encapsulated using pristine and RGD-conjugated PEG hydrogels to study their differentiation in three dimensional (3D) biomimetic environments. We hypothesized that providing cell adhesion sequences (i.e., RGD peptide) can promote the ES cell fate towards endothelial lineage, while EBs within non-adhesive pristine PEG hydrogel can show their preferential differentiation towards cardiogenic lineage. To test this hypothesis we evaluated the EB differentiation by quantifying the beating or sprouting rate as well as evaluating endothelial cell and cardiomyocyte specific gene and protein expression in PEG or RGD-conjugated PEG hydrogels.

2. Results

2.1. Characterization of EB Aggregation

Hydrogel microarrays fabricated with low molecular weight PEG-diacrylate were used for generating size-controlled mES cell aggregates (150 and 450 μm) (Figure 1A). Phase contrast microscopy images in Figure 1B show hydrogel arrays before and after seeding with mES cells. By optimizing the cell seeding density (0.3×10^6 cells for the 150 microwell chip, and 1.5×10^6 cells for the 450 microwell chip) it was possible to achieve the desired size of aggregates (150 μm-EBs and 450 μm-EBs) after a constant culture time, in this case 5 days. Subsequently, the generated EBs were collected and encapsulated in pristine high molecular weight PEG-4 arm-acrylate (Mw: 20000 Da) and in high molecular weight PEG-4 arm-acrylate conjugated with cell adhesion sequences (i.e., RGD peptide). The hydrogel area, occupied by one EB, encapsulated in pristine PEG increased along with a decrease in the number of morphologically distinguishable aggregates over time for both 450 μm (Figure 1C) and 150 μm (Figure 1D) sized EBs. Consequently, our data suggest that aggregates located within the pristine PEG were possibly interacting with each other leading to this secondary aggregation. This secondary aggregation of encapsulated EBs was reduced when cell attachment sequences (i.e., RGD peptide) were incorporated to their 3D microenvironment. The reduction in the number of aggregates encapsulated in RGD-PEG was significantly lower than in pristine PEG. The area of single EBs in RGD-PEG, regardless of its initial diameter size, did not change significantly. This difference in aggregation behavior of EBs might be due to RGD peptides in the 3D microenvironment providing cell-matrix interactions to the EBs, stabilizing them.

2.2. Cardiogenesis

Encapsulated EBs showed differences in cardiogenic differentiation depending on both their size and their microenvironment as quantified by contraction behavior, gene expression and

NIH-PA Author Manuscript

NIH-PA Author Manuscript

NIH-PA Author Manuscript

immunocytochemistry (Figure 2 and 3). Pristine PEG hydrogels allowed 450 μm-EBs to interact with each other, thereby promoting larger aggregates with spontaneous contractions.[22] In contrast, RGD conjugation resulted in decreased cardiogenic differentiation. Average number of spontaneously contracting aggregates in pristine PEG increased up to 23.19 ± 3.4% on Day 12 after encapsulation, whereas the frequency of beating aggregates was only 1.6 ± 0.8% in the RGD-conjugated hydrogels on the same day (Figure 2D).

To confirm this repressive effect of RGD peptide on cardiogenic differentiation, we examined the expression of T-Box transcription factor-5 (Tbx-5), known to be expressed in early cardiogenic embryogenesis [23] and Wnt11, a member of the WNT noncanonical pathway and inducer of cardiogenic differentiation [24] as also reported in our previous study.[19] The RT-PCR analysis showed that Tbx-5 expression of 450 μm-EBs encapsulated in pristine PEG was significantly higher ($p < 0.05$, $n = 3$) in the early days of their encapsulation (i.e., Day 3) compared to RGD-modified PEG (Figure 2C), while there was no significant difference on their Wnt11 expression. We also evaluated cardiogenic differentiation of EBs using immunocytochemistry. It was found that 450 μm-EBs encapsulated in pristine PEG hydrogels expressed sarcomeric alpha actinin (Figure 2A), whereas this marker was not detectable in RGD-PEG under the same conditions (Figure 2B). In addition, cell aggregates in RGD-PEG expressed higher CD31 than aggregates in pristine PEG. Material dependent cardiogenic differentiation was also apparent in 150 μm-EBs. As in 450 μm-EBs, spontaneously contracting 150 μm-EBs in RGD-PEG was reduced by about 5 fold compared to those in pristine PEG by Day 12 of encapsulation (Figure 3D). On the other hand, 150 μm-EBs inside PEG hydrogels showed higher aggregation with higher number of beating aggregates. Spontaneous beating started on Day 3 of encapsulation and reached its peak on Day 5 for 150 μm-EBs. Immunocytochemical analysis confirmed the effect of RGD peptide on reducing cardiogenic differentiation in 150 μm-EBs as shown by the attenuated reaction of EBs in RGD-PEG to sarcomeric alpha actinin (Figure 3B). In contrast, pristine PEG hydrogels enabled cardiogenic differentiation as further proven by positive sarcomeric alpha actinin staining (Figure 3A). Results of gene expression analysis performed on 150 μm-EBs were consistent with the quantification and immunostaining data. Tbx-5 and Wnt11 were expressed at lower levels when 150 μm-EBs were encapsulated in RGD-PEG, especially on late stages of culture (i.e., Day 12) for Tbx-5 and both early and late stages for Wnt11 (i.e., Days 3 and 12) (Figure 3C). Overall, our results suggest that RGD peptides incorporated in a 3D hydrogel environment reduced the differentiation of both EB sizes towards cardiomyogenic lineage, while pristine PEG hydrogels allowed for aggregation of EBs and spontaneous cardiogenic differentiation as shown by contracting behavior, immunohistochemistry (sarcomeric alpha actinin) and gene expression analysis (Tbx-5 and Wnt11).

2.3. Endothelialization

Based on its well-known role in vasculogenesis, [4, 11, 13] we conjugated RGD peptide in PEG hydrogels to create a biomimetic 3D microenvironment. Our results showed that RGD sequence presence has a dominant effect in driving endothelial differentiation of size-controlled EBs. 450 μm and 150 μm-EBs were encapsulated in pristine PEG or RGD-PEG hydrogels and their differentiation towards endothelial lineage was examined by quantification of their sprouting behavior, gene expression and immunocytochemistry analysis. While cardiogenic differentiation of 450 μm-EBs was reduced by incorporation of RGD peptide to pristine PEG hydrogels (Figure 2), their endothelial differentiation was significantly increased (Figure 4). Endothelial differentiation was quantified by sprouting aggregates and further characterized by immunocytochemical analysis using EC markers CD31 and VE-Cadherin for 450 μm-EBs-laden pristine PEG (Figure 4A) and RGD-PEG

NIH-PA Author Manuscript

NIH-PA Author Manuscript

NIH-PA Author Manuscript

hydrogels (Figure 4B). All aggregates in the latter were strongly stained with both markers, whereas some of the aggregates in PEG hydrogels were not (Figure 4A, marked with yellow arrow). To further analyze sprouting of 450 μm-EBs, we quantified the endothelialization behavior over 15 days in culture after encapsulation. The sprouting outgrowth could easily be identified with phase contrast microscopy, which increased over time in both, PEG and RGD-PEG in terms of the number of sprouting aggregates and the length of each sprout. Interestingly, we observed a distinct difference between both polymers in which vessel sprouting occurred in RGD-PEG 5 days prior to pristine PEG (Figure 4C and D). Phase contrast microscopy images on Day 2 of encapsulation showed different sprouting behavior between polymers (Figure 4C). Enhanced sprouting was not only observed in the appearance time of the sprouts, but also in the number of sprouting EBs with twice as much sprouting EBs in RGD-PEG compared to pristine PEG (Figure 4D). In addition, the average sprouting length of each sprout per EB in RGD-PEG was higher compared to PEG (Figure 4E). The number of sprout branching points (i.e., how many capillaries sprout out of already existing ones and out of the EB itself) was also higher in RGD-PEG (Figure S2). Furthermore, EBs surrounded by RGD-containing 3D microenvironment expressed higher levels of Wnt5a, CD31 and VE-Cadherin compared to pristine PEG environment (Figure 4F).

Endothelial differentiation was also examined for 150 μm-EBs that were encapsulated in pristine PEG and RGD-PEG hydrogels (Figure 5). Although immunocytochemistry results showed that 150 μm-EBs were positive for CD31 and VE-Cadherin in both PEG (Figure 5A) and in RGD-PEG (Figure 5B), quantification data and gene expression analysis suggested that RGD peptides enhanced endothelial cell differentiation of 150 μm-EBs. Vascularization of 150 μm-EBs in pristine PEG started three days after encapsulation. Interestingly, with RGD peptide the vessel sprouting started on Day 2 of encapsulation as shown for 450 μm (Figure 5C). Although sprouting of 150 μm-EBs appeared earlier than that of 450 μm-EBs inside pristine PEG hydrogels, when RGD peptide was added, overall sprouting was enhanced regardless of the size of encapsulated EBs. The number of sprouting 150 μm-EBs (Figure 5D) was nearly doubled, the average length of each sprout (Figure 5E) as well as the number of sprouts (Figure S2) increased significantly in RGD-PEG. The evaluation of endothelial gene expression for 150 μm-EBs in PEG vs. RGD-PEG showed a significant increase in the expression of CD31, VE-Cadherin and Wnt5a at early stages after encapsulation. Overall, the gene expression analysis showing that RGD enhances endothelialization at early stages of differentiation (Figure 4 and Figure 5: Day 3 of encapsulation) support our hypothesis in that RGD peptides provide acceleration of endothelial cell differentiation. In line with these results the decrease of cardiogenic differentiation was also significant at early stages of differentiation (Figure 2 and Figure 3). To our knowledge, the trends of gene expressions of endothelial or cardiac differentiation markers can only show generic proportions of the respective lineage cells in the EBs. Thus, we performed quantitative analyses of beating or sprouting EBs to further support our hypothesis, showing the obvious differences in differentiated cells' functions.

3. Discussion

Three-dimensional (3D) microenvironments have been shown to be useful in directing cellular development and stem cell fate.[1, 6, 25] For a number of different cell types two-dimensional (2D) culture conditions are different from the conditions to which cells are exposed inside the body, where they are associated with many different molecules and surrounded by neighboring cells. Thus in 2D culture systems only the basal region of the cell is in contact with the extracellular matrix (ECM) and neighboring cells.[12] In vivo, cells are contained within an ECM that creates a relatively soft microenvironment and high water content.[3] Given this complexity it is important to develop 3D models, since they mimic the native tissue organizations more closely.[6] However, 3D approaches can have limitations

NIH-PA Author Manuscript

NIH-PA Author Manuscript

NIH-PA Author Manuscript

especially in sustaining cell viability after the encapsulation process.[26] In this study we used Irgacure 2959 as a curing agent during UV exposure, which was shown to be tolerated by stem cells.[27]

The development of EBs is a method that has been widely used to mimic early in vivo developmental processes, which allow the differentiation of mES cells towards all the three germ layers.[28] To create in vivo-like aggregates, mES cells can be cultured on 2D flat substrates and cell aggregation can be induced over time.[29] Taking in consideration the stem cell niche, different studies have been performed to understand the effects of several parameters involved in directing stem cell fate, including the size of aggregates [18, 19] or the chemical and mechanical properties of applied materials.[26, 30] In our previous study we have shown that the size of the mES cell aggregates can direct stem cell fate towards a specific lineage. In particular, EBs with a diameter of 150 μm tended to differentiate towards ECs, while larger EBs (450 μm) differentiated towards cardiomyocytes.[19] In this work, we extended this previous study to examine the differentiation of both EB sizes in a 3D microenvironment, consisting of 4-arm PEG hydrogels, with or without conjugated RGD peptides. The encapsulation process is demonstrated in Figure S3. Previously it has been shown that inhibiting proteins important for cell adhesion such as the Scr kinase, by adding PP2 as an inhibitor, led to a decrease in EB spreading and an increase in the number of beating EBs.[31] We followed a similar strategy, but approached the problem from a different angle, such that by enhancing cell adhesion vessel sprouting should increase. Therefore, we conjugated PEG with RGD peptide that is well known for its biological role in cell adhesion and migration processes as well as in vasculogenic and angiogenic processes, [4, 30, 32] and exploited its presence to enhance endothelial lineage differentiation. PEG hydrogels consist of high water content resembling the native ECM that surrounds stem cells.[33] After 2 days in culture, further aggregation of EBs embedded in PEG was higher compared to RGD-conjugated ones, regardless of the initial size of preformed EBs. In the absence of biological signaling in their immediate surrounding, aggregates might be growing due to the tendency of the mES cells to seek cell-cell interactions.[7] Since PEG is a bio-inert hydrophilic polymer, [16, 34] it does not contain any biological signaling cues, which might have driven the cells to interact with each other. Accordingly, EB aggregation was reduced in PEG hydrogels containing cell attachment sequences (RGD peptides).

The enhanced cardiogenic differentiation in PEG compared to RGD-PEG occurred along with higher EB aggregation and lower sprouting (Figure 6). Our results are in agreement with previous studies showing that aggregation of cell clusters might promote cardiogenic differentiation.[22, 35, 36] This might also explain why cardiogenic differentiation occurred in both sized EBs, 150 μm and 450 μm-EBs. Grepin et al. also showed that ES cell aggregation induces cardiogenic differentiation, and suggested that overexpression of GATA-4, which in turn increases the expression of several cardiac markers, could explain how cell aggregation induced cardiogenic differentiation.[37] In a previous study using a similar approach to ours, single ES cells were encapsulated in RGD-conjugated PEG hydrogels.[22] Aggregation inside PEG hydrogel was observed in less than 10% of the encapsulated cells and occurred 14 days after encapsulation. In contrast, our results showed that the total number of encapsulated EBs decreased to one-third of its branching points over a 15 day period and EB aggregation started 2 days after encapsulation. Consistent with our results, the results of this study showed that cardiogenesis preferably appears in larger aggregates.

With regard to the initial size of EBs, we observed earlier endothelial differentiation of smaller EBs (initial diameter size: 150 μm) compared to larger ones (initial diameter size: 450 μm) inside PEG hydrogels which was expressed in earlier occurring sprouting (Figure 6). This result is consistent with our previous 2D study using similar sized EBs.[19] When RGD peptide was conjugated to PEG hydrogels, EB aggregation decreased along with

NIH-PA Author Manuscript

NIH-PA Author Manuscript

NIH-PA Author Manuscript

cardiogenic differentiation. Simultaneously, ES cell differentiation towards ECs was accelerated and increased over time. EB sprouting represents the differentiation towards ECs and the formation of a de novo vasculogenic system. The number of sprouting EBs, the number of sprout branching points, and the length of each sprout were higher in RGD-PEG than in PEG. So far, many successful approaches to enhance endothelialization have been tried.[13] However, there are still some essential limitations in their application. For instance, the usage of cytokines and growth factors as additional supplements, such as VEGF, PDGF, or transforming growth factor beta (TGF-β), to enhance vasculogenesis were shown to be a successful strategy to induce neovascularization in engineered tissues. However, this strategy led to uncontrolled vasculogenesis. Thus, applying soluble factors in vivo did not succeed because of the low bioavailability. This is due to the high degradation rate of these costly growth factors after injection. Consequently, a long term effect could not be achieved.[3, 5]

To overcome these limitations, a promising approach is to modify inert biomaterials with protein or peptide sequences known to promote vasculogenesis. For example, the effect of VEGF on EC differentiation was evaluated in a study using human ES (hES) cells.[38] In this study hES cell aggregates, previously grown in VEGF-containing EGM media were encapsulated inside dextran-based hydrogels, containing VEGF-loaded microparticles or conjugated with RGD. They showed that neither the incorporation of VEGF particles, nor the conjugation with RGD peptides enhanced endothelialization in these gels. However, RGD peptides did improve cell adhesion and EC differentiation in 2D when hES cells were seeded onto RGD-containing dextran hydrogels. The positive effect of VEGF towards endothelialization appeared after isolating cell aggregates from VEGF microparticle-containing dextran hydrogels and subsequently replating the cell aggregates onto a 2D surface with VEGF-containing EGM media. In contrast, we show that in the system presented here the presence of RGD peptides resulted in directed EC differentiation from different sized EBs inside PEG hydrogels, even when cultured in basic EB media, without the addition of further supplements. The missing effect of those adhesive sequences in this study can be due to the fact, that cell aggregates were grown in EGM media prior to encapsulation, which might have pre-dominated the effect of VEGF and RGD. Another reason could be the time point of encapsulation: aggregates were encapsulated after 10 days of culture. VEGF and RGD might have their promoting effect at earlier stages of differentiation. For instance, our results show that endothelial gene expression is enhanced at a statistically significant degree in RGD-PEG hydrogels at early stages of differentiation, when compared to PEG. The effect of the plating time on cell fate has not been studied in details, but a recent study showed that the time of plating EBs can influence their differentiation.[39]

In this study CD31, VE-Cadherin and Wnt5a were used to characterize endothelial cell differentiation by gene expression analysis. CD31 as endothelial junction protein was shown to be expressed in early stages of ES cell differentiation towards endothelial lineage.[40] In the same study, VE-Cadherin was shown to be expressed at later stages of differentiation. Wnt5a was chosen as an additional marker for endothelial cell differentiation for its crucial role in endothelial cell differentiation derived from ES cells.[41]

We speculate that the porous structure of the polymer might have led to enhanced cell-cell interaction in 4-arm PEG lacking adhesive ligands. This is allowed by the 4-arm structure that was initially designed with the aim to enhance cell-interactions.[17, 42] Previous studies have suggested that the PEG-arms allow interactions between cells and adhesive peptides in a biospecific manner via receptor-ligand interactions. In our case, the RGD peptides are the ligands for binding to integrin-receptors expressed on the cell surface. In comparison, they suggest that spacer (arm)-free PEG hydrogels do not provide sterical availability of the

NIH-PA Author Manuscript

NIH-PA Author Manuscript

NIH-PA Author Manuscript

incorporated peptide, which presumably leads to non-specific cell adhesion and undesired protein adsorption.[43] Thus, these findings substantiate our results. The spacers inside 4-arm PEG hydrogels presumably enhance cell migration allowing for cell-cell interaction inside a non-biological microenvironment resulting in aggregation. The high aggregation trend showed a supportive role towards cardiogenic differentiation, but also allowed endothelialization through spontaneous differentiation. The incorporation of RGD peptides allowed the interaction between the cells and their microenvironment, leading to preferred differentiation towards ECs, which can be explained by the distinct role of RGD peptides in vasculogenic and angiogenic processes.

Although the pore size of PEG hydrogels was previously shown to be in the nanometer range, [44] other studies [45] analyzed the effect of increasing the molecular weight on the pore size, providing evidence about increased pore size when increasing the molecular weight of PEG hydrogels. In addition, PEG acrylate hydrogels are hydrolytically degradable.[46] This might further explain the sprouting behavior by encapsulated EBs.

4. Conclusion

In conclusion, our results suggest that the RGD peptide incorporated in a 3D hydrogel microenvironment can support mES cell differentiation towards the endothelial lineage, while EBs encapsulated in pristine PEG hydrogels have more tendency to differentiate towards a cardiogenic lineage. This was demonstrated on different sized-EBs derived from aggregating mES cells that were previously formed using microwell arrays. Independent of EB size, RGD peptides led to reduce EB aggregation, which in turn resulted in reduced cardiogenesis, as well as enhanced endothelial differentiation. On the other hand, EBs encapsulated in pristine PEG hydrogels showed an increase in their cardiogenic differentiation. We expect these findings to be especially important given that the photolabile approach we used in this study allows for spatial patterning of ES cell-laden plain and RGD-conjugated PEG hydrogels, which can potentially be used to induce vessel sprouting in a controlled manner. Advances in these approaches can lead to improve methodologies for tissue regeneration purposes with the aim of restoring vessel formation in damaged tissues in vivo.

5. Experimental Section

Microwell Fabrication

Micropatterned wells with 150 μm and 450 μm diameters were fabricated using a silicon wafer and a poly(dimethylsiloxane) (PDMS) mold as described previously.[20] PDMS molds were prepared with silicone elastomer base and curing agent (Sylgard 184, Essex Chemical), which were mixed in a 10:1 ratio. Fabricated PDMS molds with protruding columns that were 150 μm and 450 μm in diameter were peeled from the silicon wafer and used as stamps to generated PEG microwells. To fabricate the microwells, 10% PEG-dimethacrylate (wt/v, 1000 Da, polysciences Inc.) solution containing 1% photoinitiator (wt/v, Igracure 2959, BASF, Ludwigshafen, Germany) was crosslinked via UV exposure (intensity: 100 mW/cm^2, final power: 750 mW) on glass slides. Glass slides and PDMS molds were sterilized with ethanol prior to being used. Microwells were stored in PBS at 37 °C overnight before seeding ES cells.

ES Cell Culture and EB Formation

Murine embryonic stem cells (mES cells - R1 cell line, produced by crossing two 129 mouse substrains: 129S1/SvlmJ and 129 × 1/Svj, ATCC) derived from the inner cell mass of a 3.5 day aged mouse blastocyst were cultured in a high glucose - Dulbecco's Modified Eagles Medium (DMEM) (ATCC SCRR-2010) supplemented with 10% ES cell qualified-fetal

NIH-PA Author Manuscript

NIH-PA Author Manuscript

NIH-PA Author Manuscript

bovine serum (ES-FBS) (Gibco), L-Alanyl-L-Glutamine (2.0 mM, ATCC 30-2115), 2-mercaptoethanol (0.1 mM, Invitrogen Life Technologies), and mouse leukemia inhibitory factor (LIF, 1000 U/ml) (Chemicon) at 37 °C and 5% carbon dioxide. mES cells were cultured using 0.1% gelatin (from porcine skin, Sigma-Aldrich) coated flasks, and LIF containing media changed daily.

mES cell seeding density was optimized to 0.3×10^6 cells/150 μm-chip and 1.5×10^6 cells/450 μm-chip to obtain the optimal amount of cells inside the microwells (chips for both size EBs were ca. 1 cm^2). After seeding, samples were washed with media to remove cell residues (i.e., cells resting in the interspaces between the wells). Seeded microwells were cultured in EB media (alpha Minimal Essential Medium (α-MEM; Gibco) supplemented with 15% heat inactivated FBS (Gibco), 1% penicillin/streptomycin) under 5% CO_2 at 37 °C for 5 days. Media was changed daily, starting on Day 2 of culture. On Day 6, mEC cells aggregates that were formed inside microwells of different diameter sizes (150 and 450 μm) were collected and used for encapsulation.

RGD-Conjugation in PEG-polymer

To create cell adhesive 3D microenvironments within PEG-Acrylate (4arm PEG Acrylate, MW: 20000 Da, JenKem Technology) hydrogels, the peptide sequence YRGDS (H-tyr-Arg-Gly-Asp-Ser-OH, Mw 596.60, Bachem) was conjugated to acryloyl-PEG-N-hydroxysuccinimide (acryl-PEG-NHS, Mw 3400, Jen Kem Technology) as described previously.[21] The yield of the conjugation reaction was analyzed with Nuclear Magnetic Resonance (H-NMR) - Spectroscopy (Figure S1). RGD-PEG-3400 acryl was added in a 1:10 molar ratio to 4-arm PEG during the encapsulation step.

EB Encapsulation

EBs of different sizes (150 and 450 μm) were collected from the microwells after 5 days of culture and encapsulated in 10% (wt/v) 4-arm PEG-acrylate or in 4-arm PEG-acrylate and RGD-conjugated PEG-acrylate mixture using 0.1% (wt/v) Irgacure 2959. Single EBs were collected with colorless DMEM (Gibco) by gently pipetting on the top of the microwell array, collected in 15 mL conical tubes and kept for 10 min allowing the EBs to settle down. After removing the residual media, a double concentrated (20% PEG or RGD-PEG polymer in 0.2% Irgacure 2959) polymer solution was mixed in a 1:1 volume ratio with collected EBs that were resuspended in colorless DMEM to obtain a final concentration of 10% polymer solution with 0.1% Irgacure 2959, and crosslinked via UV-exposure for 30 sec. (intensity: 12 mW/ cm^2, final power: 800 mW). This was achieved by mixing the pre-polymer solution with EB containing colorless DMEM right before every exposure. The sample thickness was regulated according to the EB size and controlled by spacers to obtain 450 μm and 600 μm thick hydrogels for 150 μm and 450 μm-EBs respectively. EB-laden hydrogels were cultured in EB media for 15 days at 37 °C under 5% CO_2. Starting with Day 4, 50% of the media was changed every second day. The encapsulation day is referred to as “Day 0”, which corresponds to Day 6 of the cell aggregation. mES cells were cultured for a total of 20 days, 5 days in microwell arrays, and 15 days after encapsulation.

Number of Beating EBs

Cardiogenic differentiation was quantified by counting the number of beating colonies every other day throughout the 15 days of encapsulation using an inverted cell culture microscope (Nikon Eclipse). Number of beating aggregates was normalized to the total number of aggregates at each time point. A total of around 200 single EBs was used to encapsulate 450 μm-EBs, and about 160 single EBs with a diameter of 150 μm were encapsulated within one sample. All quantification experiments and analysis were performed using at least three independent samples and the measurements were performed using ImageJ (NIH, USA).

NIH-PA Author Manuscript

NIH-PA Author Manuscript

NIH-PA Author Manuscript

Quantification of Sprouting EBs

EBs sprouting was quantified every other day for 15 days and data was collected and normalized as described above. In addition, the length of sprouts generated from each EB was measured and the number of the branching points of the sprouts was counted. Each sprout that comes out of an already existing one was counted as a new branching point. The length and the number of branching points per sprouting EB were added up to result in a mean value for each EB.

Reverse Transcription–Polymerase Chain Reaction (RT-PCR)

RT-PCR was performed on Days 3, 7 and 12 of encapsulation (which is Day 8, 12 and 17 starting from cell seeding in microwells) to evaluate the differentiation of encapsulated EBs in pristine PEG and RGD-PEG hydrogels through gene expression. RNA was isolated with a RNA-isolation KIT (RNeasy Mini Kit, Qiagen) according to the manufacturer´s instructions. To examine cardiogenic gene expression Tbx-5 and Wnt11 were examined. Furthermore, to assess endothelial specific gene expression CD31, VE-cadherin and Wnt5a was screened. The synthesis of cDNA and PCR amplification was performed using SuperScript™ III One-Step RT-PCR System with Platinum Taq (Invitrogen). RNA (50 ng) was used to synthesize cDNA at 55 °C and 20 min, which was then amplified by several cycles using a PTC-100TM thermal cycler (MJ Research Inc). The cycle conditions were 15 sec denaturation at 95 °C, 30 sec primer annealing temperature, and 45 sec extension at 68 °C. After PCR amplification, the DNA product was loaded on 1% (wt/wt) agarose gel, with ethidium bromide (0.4 μg/ mL) and gel electrophoresis was performed for 5 min at 50 V, followed by an additional 15 min at 100 V.

Immunocytochemistry

Samples containing cell aggregates were fixed with paraformaldehyde (4%, Sigma) for 1.5 h at room temperature (RT) and incubated in Triton X-100 (0.1%, Sigma) 45 min at RT to induce permeabilization. In between each step, gels were washed for several times with PBS. To inhibit unspecific binding, samples were blocked with 5% horse serum in PBS for 1.5 hours. The primary antibodies (i.e., mouse anti-CD31 (Abcam), mouse anti-VE-Cadherin (Abcam), or rabbit anti-sarcomeric alpha actinin (Abcam)) were incubated overnight at 4 °C, in a dilution of 1:100 in 5% horse serum. Subsequently, samples were washed thoroughly with PBS, and the secondary antibodies were added in a 1:200 dilution in 5% horse serum and incubated overnight at 4 °C. The fluorescently active secondary antibodies were Alexa Fluor 546 anti-rabbit IgG (Invitrogen) and Alexa Fluor 488 goat anti-mouse IgG (Invitrogen). To visualize cell nuclei, DAPI containing mounting solution (ProLong Gold antifade reagent w/DAPI, Invitrogen) was used.

Statistical Analysis

All quantifications were done using at least 3 independent samples from at least two independent experiments, and error bars represent standard deviation. RT-PCR analyses were performed based on the band intensity measurements of multiple trials and error bars represent standard deviation. Statistical significance was determined using one-way ANOVA followed by Tukey’s Multiple Comparison Test for $p < 0.05$.

Supplementary Material

Refer to Web version on PubMed Central for supplementary material.

NIH-PA Author Manuscript

NIH-PA Author Manuscript

NIH-PA Author Manuscript

Acknowledgments

Lina Schukur was supported by the German Academic Exchange Service (DAAD) and by Ms Elizabeth Meurer. This paper was supported by the Institute for Soldier Nanotechnology, National Institutes of Health (HL092836, DE021468, DE019024, EB012597, EB008392, HL099073), the National Science Foundation (DMR0847287) and the Office of Naval Research Young Investigator award.

References

1. Khademhosseini A, Vacanti JP, Langer R. Sci. Am. 2009; 300:64. [PubMed: 19438051]
2. Moon JJ, Saik JE, Poche RA, Leslie-Barbick JE, Lee S-H, Smith AA, Dickinson ME, West JL. Biomaterials. 2010; 31:3840. [PubMed: 20185173]
3. Santos MI, Reis RL. Macromol. Biosci. 2010; 10:12. [PubMed: 19688722]
4. Bellis SL. Biomaterials. 2011; 32:4205. [PubMed: 21515168]
5. Lovett M, Lee K, Edwards A, Kaplan DL. Tissue Eng. 2009; 15:353.
6. Kraehenbuehl TP, Langer R, Ferreira LS. Nat. Methods. 2011; 9:731. [PubMed: 21878920]
7. Guilak F, Cohen DM, Estes BT, Gimble JM, Liedtke W, Chen CS. Cell Stem Cell. 2009; 5:17. [PubMed: 19570510]
8. Rouwkema J, Gibbs S, Lutolf MP, Martin I, Vunjak-Novakovic G, Malda J. J. Tissue Eng. Regen. Med. 2011; 5:164.
9. Matsuura K, Masuda S, Haraguchi Y, Yasuda N, Shimizu T, Hagiwara N, Zandstra PW, Okano T. Biomaterials. 2011; 32:7355. [PubMed: 21807408]
10. Ye Z, Zhou Y, Cai H, Tan W. Adv. Drug Delivery Rev. 2011; 63:688.
11. Shachar M, Tsur-Gang O, Dvi T, Leor J, Cohen S. Acta Biomater. 2011; 7:152. [PubMed: 20688198]
12. Lutolf MP, Gilbert PM, Blau HM. Nature. 2009; 462:433. [PubMed: 19940913]
13. Novosel EC, Kleinhans C, Kluger PJ. Adv. Drug Delivery Rev. 2011; 63:300.
14. Vunjak-Novakovic G, Scadden DT. Cell Stem Cell. 2011; 8:252. [PubMed: 21362565]
15. Lee SH, Miller JS, Moon JJ, West JL. Biotechnol. Prog. 2005; 21:1736. [PubMed: 16321059]
16. Raeber GP, Lutolf MP, Hubbell JA. Biophys. J. 2005; 89:1374. [PubMed: 15923238]
17. Lutolf MP, Raeber GP, Zisch AH, Tirelli N, Hubbell JA. Adv. Mater. 2003; 18:888.
18. Bauwens CL, Peerani R, Niebruegge S, Woohdhouse KA, Kumacheva E, Husain M, Zandstra PW. Stem Cells. 2008; 26:2300. [PubMed: 18583540]
19. Hwang Y-S, Chung BG, Ortmann D, Hattori N, Moeller H-C, Khademhosseini A. Proc. Natl. Acad. Sci. U. S. A. 2009; 106:16978. [PubMed: 19805103]
20. Moeller H-C, Mian MK, Shrivastava S, Chung BG, Khademhosseini A. Biomaterials. 2008; 29:75263.
21. Gobin AS, West JL. FASEB J. 2002; 16:751. [PubMed: 11923220]
22. Kraehenbuehl TP, Zammaretti P, Vlies AJVd, Schoenmakers RG, Lutolf MP, Hubble JA. Biomaterials. 2008; 29:2757. [PubMed: 18396331]
23. Bruneau BG, Nemer G, Schmitt JP, Charron F, Robitaille L, Caron S, Conner DA, Gessler M, Nemer M, Seidman CE, Seidman JE. Cell. 2011; 106:709. [PubMed: 11572777]
24. Terami H, Hidaka K, Katsumata T, lio A, Morisaki T. Biochem. Biophys. Res. Commun. 2004; 325:968. [PubMed: 15541384]
25. Kraehenbuehl, TP. Ch. 3. In: Aday, S.; Ferreira, LS., editors. Biomedical Engineering, Vol. 10. Heidelberg, Germany: Springer; 2011.
26. Zustiak SP, Durbal R, Leach JB. Acta Biomater . 2010; 6:3404. [PubMed: 20385260]
27. Williams CG, Malik AN, Kim TK, Manson PN, Elisseeff JH. Biomaterials. 2005; 26:1211. [PubMed: 15475050]
28. Itskovitz-Eldor J, Schuldiner M, Karsenti D, Eden A, Yanuka O, Amit M, Soreq H, Benvenisty N. Mol. Med. 2000; 6:88. [PubMed: 10859025]
29. Dang SM, Gerecht-Nir S, Chen J, Itskovitz-Eldor J, Zandastra PW. Stem Cells. 2004; 22:275. [PubMed: 15153605]

NIH-PA Author Manuscript

NIH-PA Author Manuscript

NIH-PA Author Manuscript

30. Fuchs C, Scheinast M, Paseiner W, Lagger S, Hofner M, Hoellrigl A, Schultheis M, Weitzer G. Cells Tissues Organs. 2011; 6:1.
31. Hakuno D, Takahashi T, Lammerding J, Lee RT. The J. Biol. Chem. 2005; 280:39534.
32. Guarnieri D, Capua AD, Ventre M, Borzacchiello A, Pedone C, Marasco D, Ruvo M, Netti PA. Acta Biomater. 2010; 6:2532. [PubMed: 20051270]
33. Liu SQ, Tay R, Khan M, Ee PLR, HendrickL JL, Yang YY. Soft Matter. 2010; 6:67.
34. Chan V, Zorlutuna P, Jeong JH, Kong H, Bashir R. Lab Chip. 2010; 10:2062. [PubMed: 20603661]
35. Skerjanc IS, Slack RS, McBurney WM. Mol. Cell. Biol. 1994; 14:8451. [PubMed: 7969178]
36. Smith SC, Reuhl KR, Craig J, McBurney MW. J. Cell. Physiol. 1987; 131:74. [PubMed: 2437131]
37. Grepin C, Nemer G, Nemer M. Development. 1997; 124:2387. [PubMed: 9199365]
38. Ferreira LS, Gerecht S, Fuller J, Shieh HF, Vunjak-Novakovic G, Langer R. Biomaterials. 2007; 28:2706. [PubMed: 17346788]
39. Chen M, Lin Y-Q, Xie S-L, Wu H-F, Wang J-F. Biotechnol. Lett. 2011; 33:853. [PubMed: 21165673]
40. Vittet D, Prandini M-H, Berthier R, Schweitzer A, Martin-Sisteron H, Uzan G, Dejana E. Blood. 1996; 88:3424. [PubMed: 8896407]
41. Yang D-H, Yoon J-Y, Lee S-H, Bryja V, Andersson ER, Arenas E, Kwon Y-G, Choi K-Y. Circ. Res. 2008; 104:372. [PubMed: 19096028]
42. Zhao, X.; Zhao, Y. China: Beijing Jenkem Technology Co., Ltd.; 2011. 2 360 203 A1
43. Miller JS, Shen CJ, Legant WR, Baranski JD, Bakely BL, Chen CS. Biomaterials. 2010; 31:3736. [PubMed: 20138664]
44. Raeber GP, Lutolf MP, Hubbell JA. Acta Biomater. 2007; 3:615. [PubMed: 17572164]
45. Zuo D-Y, Xu Y-Y, Xu W-L, Zuo H-T. Chin. J. Chem. Sci. 2008; 26:405.
46. Shikanov A, Smith RM, Xu M, Woodruff TK, Shea LD. Biomaterials. 2011; 32:2524. [PubMed: 21247629]

NIH-PA Author Manuscript
NIH-PA Author Manuscript
NIH-PA Author Manuscript

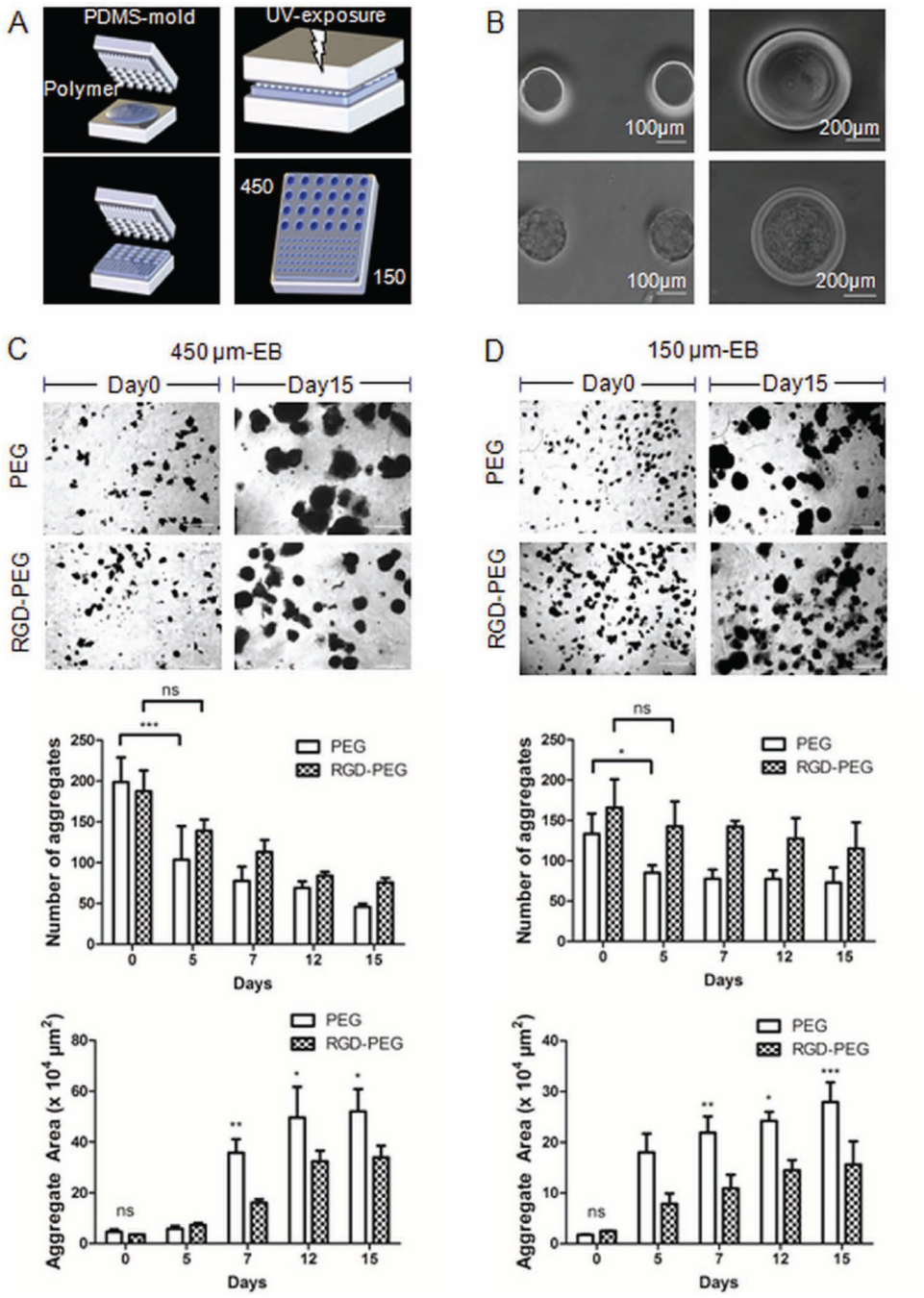

Figure 1.

Formation of Embryoid bodies (EBs) derived from murine ES cells. (A) Different sized microwell arrays (150 μm and 450 μm in diameter) were fabricated using poly(ethylene glycol) (PEG, 1 kDa) and polydimethylsiloxane (PDMS) molds under UV exposure. Phase contrast microscopy images (B) microwells with a diameter size of 150 μm (Left, scale bar: 100 μm) or 450 μm (Right, scale bar: 200 μm). Upper panel: microwells without cells, lower panel: cell-seeded microwells. (ES cell seeding density: 0.3×10^6 cells/ 150 microwell chip, and 1.5×10^6 cells/ 450 microwell chip). (C) Phase contrast microscopy of encapsulated 450 μm-EBs in 4-arm PEG (upper panel) and in RGD-PEG (lower panel) at days 0 and, day 15 (Scale bar: 1 mm). Decreased aggregation of encapsulated EBs in RGD-PEG polymer was

NIH-PA Author Manuscript

NIH-PA Author Manuscript

NIH-PA Author Manuscript

observed compared to unmodified PEG polymer. Upper graph: Reduced number of encapsulated aggregates with significant difference at early time points of encapsulation. Lower graph: Increased area in μm^2 per EB. Area measurements were performed with imageJ. The area of 20 EBs within one sample was measured to obtain a single value per EB and sample. Demonstrated results compare aggregation development in PEG and RGD-PEG. (D) Phase contrast microscopy of encapsulated EBs in PEG (upper panel) and RGD-PEG (lower panel) at days 0 and day 15 with initial diameter size of 150 μm (Scale bar: 1 mm). The decrease of the number of encapsulated EBs, along with the increase of the area per EB with initial size of 150 μm is more pronounced in PEG than in RGD-PEG. Mean area in μm^2 per aggregate in PEG vs. RGD-PEG ± SD (n = 3, * indicates $P \leq 0.05$ compared to RGD-PEG).

NIH-PA Author Manuscript
NIH-PA Author Manuscript
NIH-PA Author Manuscript

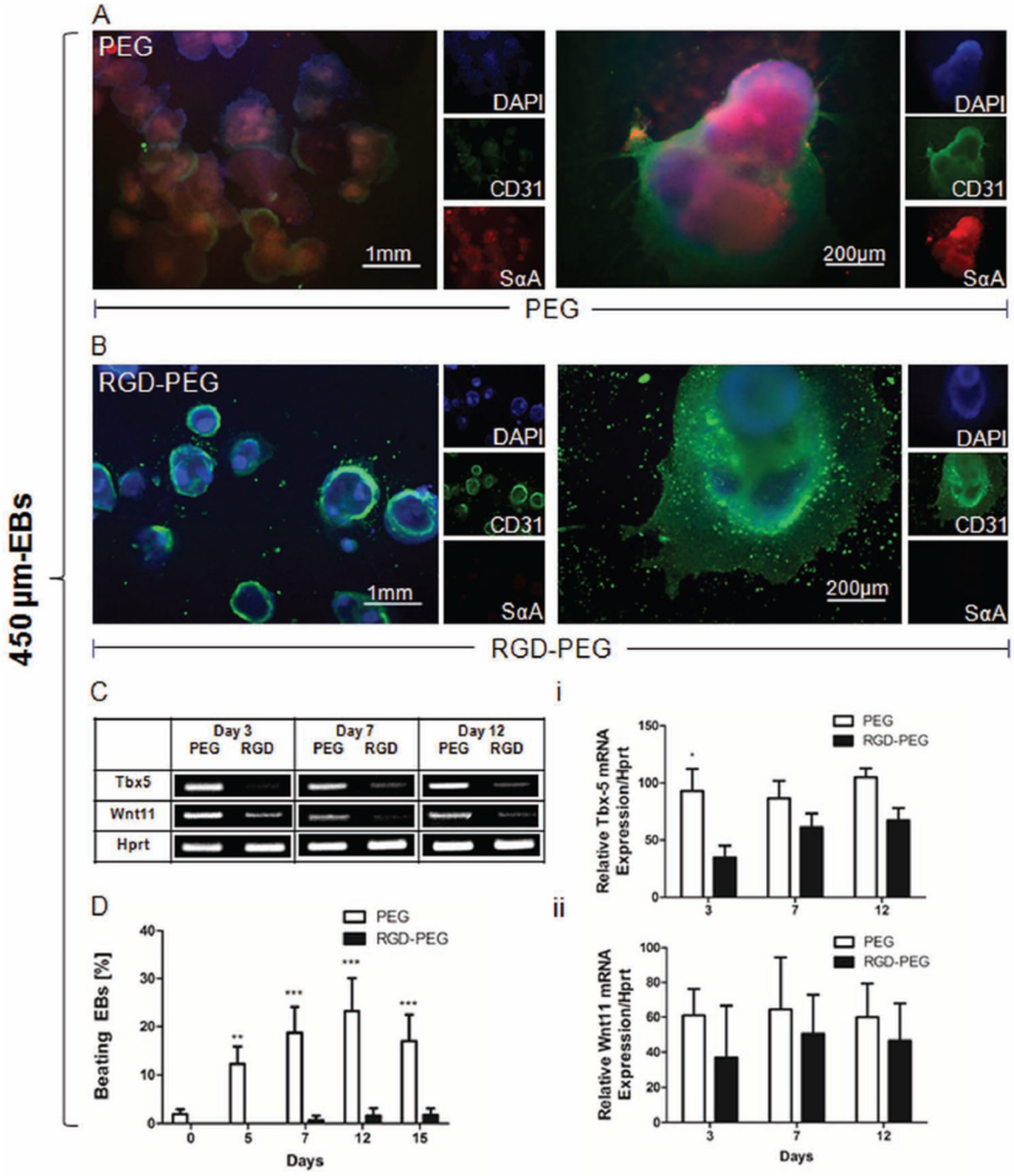

Figure 2.

Downregulation of cardiogenic differentiation in 450 μm-EBs through RGD-conjugation in 4-arm PEG. Encapsulated EBs in PEG or RGD-PEG were cultured for 15 days. (A) Immunocytochemical characterization of cardiogenic differentiation (alpha sarcomeric actinin) vs. endothelial cell differentiation (CD31) at different magnifications in PEG and (B) in RGD-PEG at day 15 of encapsulation. (C) Gel pictures: RT-PCR to characterize cardiogenic differentiation over time. (I) Tbx5 RNA expression and (II) Wnt11 RNA expression, normalized to the RNA expression of Hprt. (D) Number of beating EBs was counted over time in PEG or RGD-PEG and normalized to the number of encapsulated EBs

(aggregates) on the corresponding day (n = 3, * indicates $P \leq 0.05$ compared to RGD-PEG). Error bars without * do not represent statistical significance.

NIH-PA Author Manuscript
NIH-PA Author Manuscript
NIH-PA Author Manuscript

NIH-PA Author Manuscript
NIH-PA Author Manuscript
NIH-PA Author Manuscript

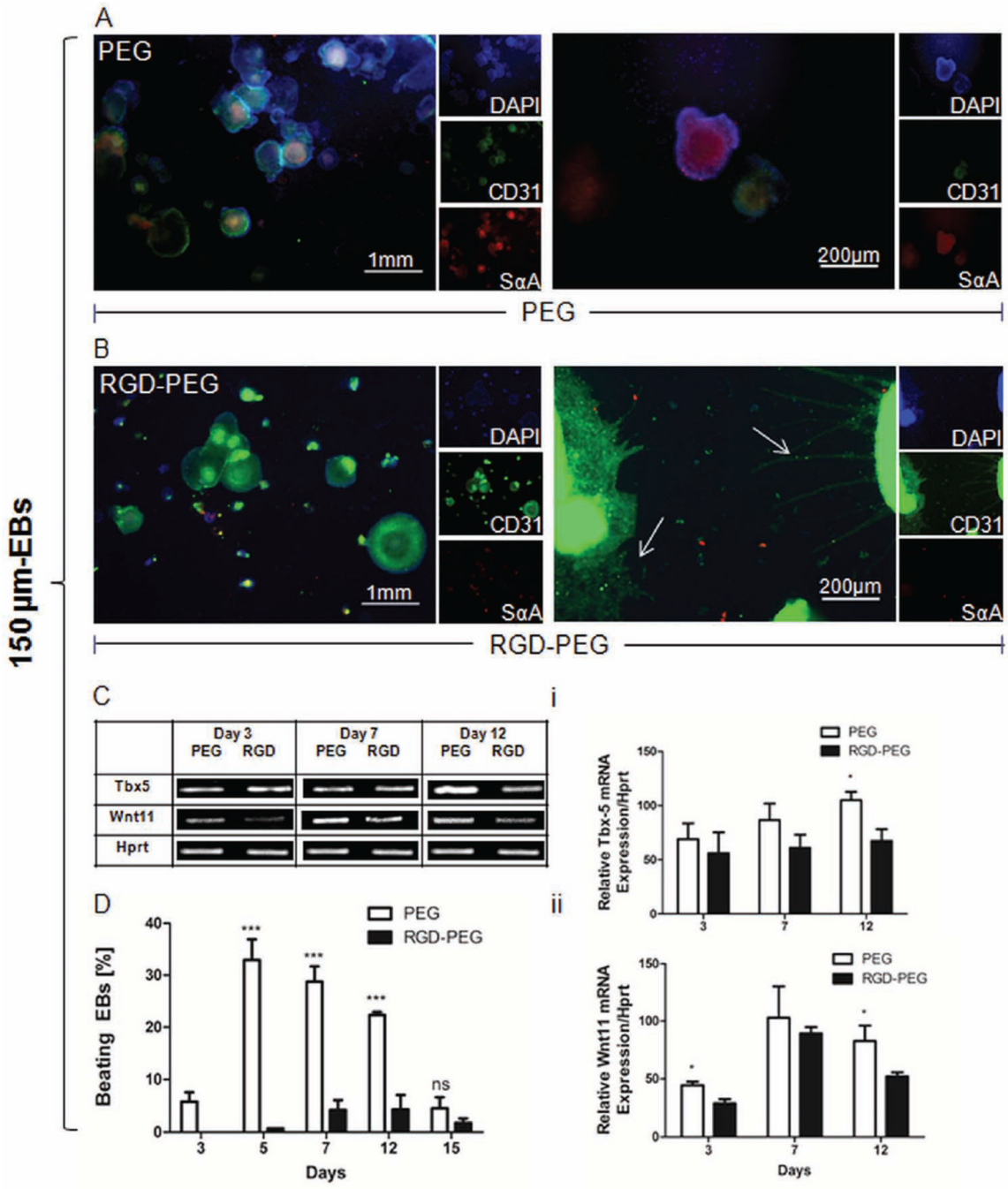

Figure 3.

Downregulation of cardiogenic differentiation in 150 μm-EBs with RGD-conjugation in 4-arm-PEG. EBs were encapsulated in PEG or RGD-PEG and cultured for 15 days as in Figure 2. (A) Immunocytochemical characterization of cardiogenic differentiation (alpha sarcomeric actinin) vs. endothelial differentiation (CD31) in PEG and (B) in RGD-PEG at day 15 of encapsulation. Arrows indicate sprouting areas. (C) Gel pictures: RT-PCR to characterize cardiogenic differentiation over time. (I) Tbx5 RNA expression and (II) Wnt11 RNA expression, normalized to the RNA expression of Hprt. (D) Number of beating EBs was counted over time in PEG or RGD-PEG and normalized to the number of encapsulated

EBs (aggregates) on the corresponding day (n = 3, * indicates $P \leq 0.05$ compared to RGD-PEG). Error bars without * do not represent statistical significance.

NIH-PA Author Manuscript
NIH-PA Author Manuscript
NIH-PA Author Manuscript

NIH-PA Author Manuscript
NIH-PA Author Manuscript
NIH-PA Author Manuscript

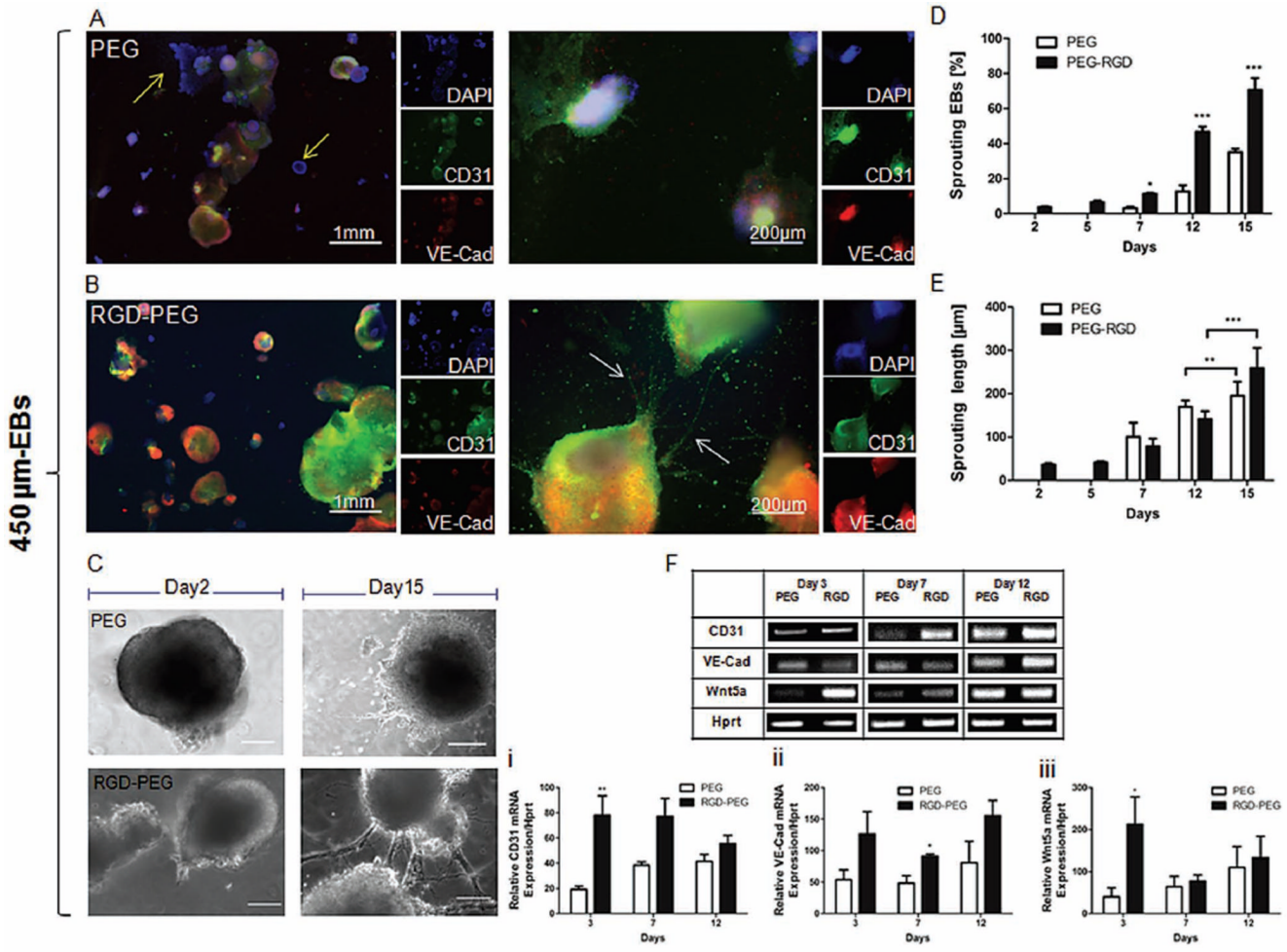

Figure 4.

Enhanced endothelialization in 450 μm-EBs with RGD-conjugation. (A) Immunocytochemical characterization of vasculogenic markers (CD31 or VE-Cadherin) in unmodified PEG polymer (Arrow indicates CD31- and VE-Cadherin- unstained areas) and (B) in RGD-PEG (Arrows indicate sprouting areas). (C) Phase contrast microscopic images of encapsulated EBs in PEG at day 2 (no sprouting visualized) and day 15. Sprouting in RGD-PEG started at day 2 of encapsulation (5 days earlier than in unmodified PEG). (Scale bars for day 2: 100 μm, day 15: 200 μm). (D)% of sprouting EBs with initial diameter size of 450 μm. The number of sprouting EBs was counted in time course and normalized to the number of encapsulated EBs. (E) Length measurements of sprouts were performed with imageJ. Values refer to the development of the length per one sprout and EB. Starting by the following time point, sprouts with a length less than 100 μm were taken out of consideration. Sprouting was visualized with phase contrast microscopy. (F) Gene expression analysis on 450 μm-EBs in PEG vs. RGD-PEG; Housekeeping gene (Hprt) and endothelial cell markers (CD31, Wnt5a, and VE-Cadherin) were screened on 450 μm-EBs at day 3, day 7, and day 12 of encapsulation (n = 3, * indicates $P \leq 0.05$ compared to RGD-PEG). Error bars without * do not represent statistical significance.

NIH-PA Author Manuscript
NIH-PA Author Manuscript
NIH-PA Author Manuscript

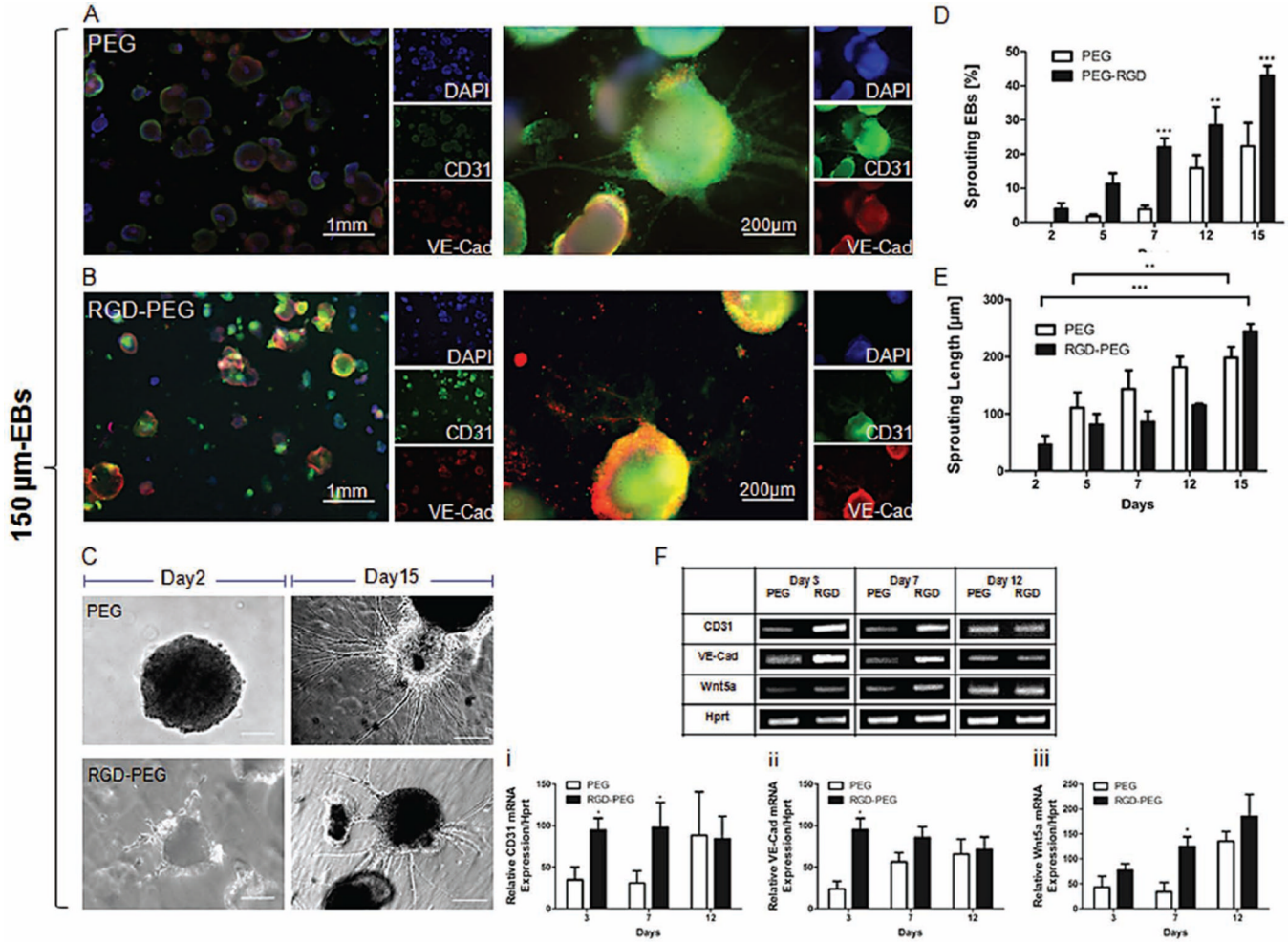

Figure 5.

Enhanced endothelialization in 150 μm-EBs through RGD-conjugation in 4-arm PEG. (A) Immunocytochemical characterization of vasculogenic markers (CD31 or VE-Cadherin) in unmodified PEG and (B) in RGD-PEG. (C) Phase contrast microscopic images of encapsulated EBs in PEG at day 2 (no sprouting visible) and day 15. Sprouting in RGD-PEG appeared 3 days earlier than in PEG. (Scale bars: 200 μm). (D)% of sprouting EBs with initial diameter size of 150 μm. The number of sprouting EBs was counted in time course and normalized to the number of encapsulated EBs. (E) Length measurements of sprouts were performed with imageJ as described in Figure 4. (F) Gene expression analyses on 150 μm-EBs in PEG vs. RGD-PEG; Housekeeping gene (Hprt) and endothelial cell markers (CD31, Wnt5a, and VE-Cadherin) were screened on 150 μm-EBs at day 3, day 7, and day 12 of encapsulation (n = 3, * indicates $P \leq 0.05$ compared to RGD-PEG). Error bars without * do not represent statistical significance.

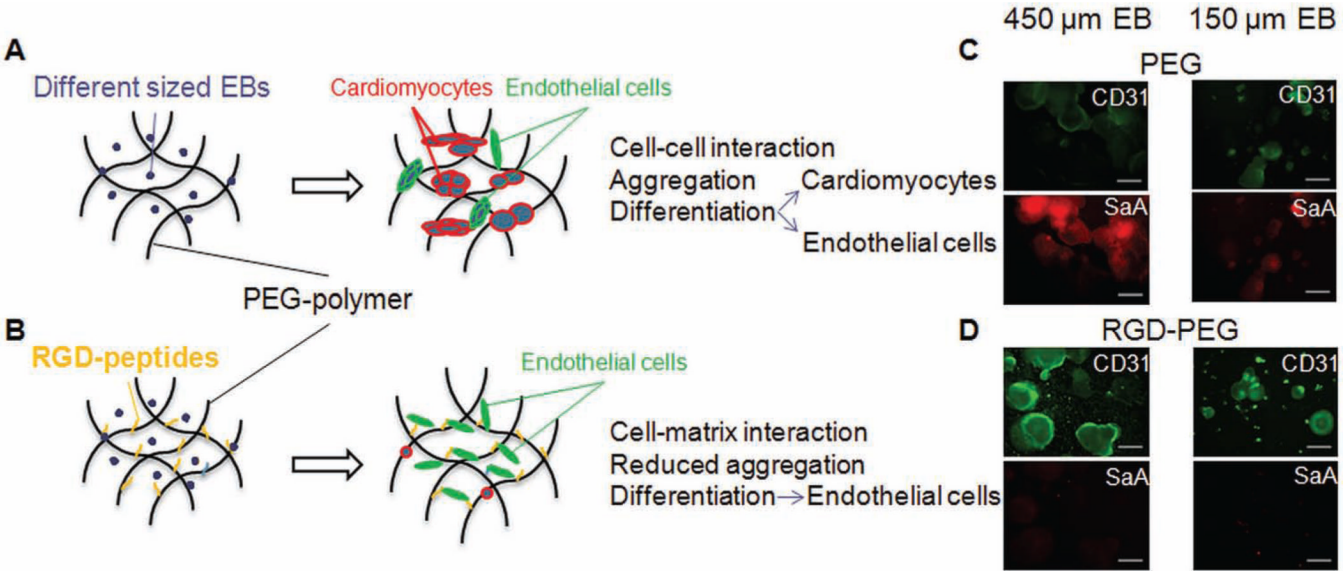

Figure 6.

(A) Schematic structure of PEG polymer containing EBs of different sizes. After culturing samples in PEG polymer, aggregation was visualized in both EB-sizes. Immunocytochemical-, gene expression-, and quantification data showed that EBs in PEG can differentiate towards cardiomyocytes and endothelial cells. (B) RGD-peptides were conjugated in PEG polymer. EBs in RGD-PEG showed lower aggregation, by increased differentiation towards endothelial cells and decreased differentiation towards cardiomyocytes. (C) Immunocytochemical staining of EBs (450 µm left and 150 µm right) encapsulated in PEG polymer. EBs expressed cardiogenic marker Sacromeric alpha actinin and endothelial marker CD31. (D) Different sized EBs embedded in RGD-PEG showed higher expression of CD31 and a significant decrease of Sacromeric alpha actinin expression. Scale bars (C, D): 500 µm.

NIH-PA Author Manuscript
NIH-PA Author Manuscript
NIH-PA Author Manuscript